

Numerical analysis of thermal post-buckling strength of laminated skew sandwich composite shell panel structure including stretching effect

Pankaj V. Katariya and Subrata Kumar Panda*

Department of Mechanical Engineering, National Institute of Technology Rourkela, Odisha, India

(Received October 9, 2019, Revised November 29, 2019, Accepted November 30, 2019)

Abstract. The computational post-buckling strength of the tilted sandwich composite shell structure is evaluated in this article. The computational responses are obtained using a mathematical model derived using the higher-order type of polynomial kinematic in association with the through-thickness stretching effect. Also, the sandwich deformation behaviour of the flexible soft-core sandwich structural model is expressed mathematically with the help of a generic nonlinear strain theory i.e. Green-Lagrange type strain-displacement relations. Subsequently, the model includes all of the nonlinear strain terms to account the actual deformation and discretized via displacement type of finite element. Further, the computer code is prepared (MATLAB environment) using the derived higher-order formulation in association with the direct iterative technique for the computation of temperature carrying capacity of the soft-core sandwich within the post-buckled regime. Further, the nonlinear finite element model has been tested to show its accuracy by solving a few numerical experimentations as same as the published example including the consistency behaviour. Lastly, the derived model is utilized to find the temperature load-carrying capacity under the influences of variable factors affecting the soft-core type sandwich structural design in the small (finite) strain and large deformation regime including the effect of tilt angle.

Keywords: post-buckling; sandwich; skew; HSDT; thermal loading; FEM

1. Introduction

The laminated composite and the sandwich structure/structural components are highly desirable in aeronautical, space and automobile industries due to their exceptional properties. In general, the sandwich-type of constructions are adopted for the design of the high-speed and reusable launch vehicles, which allows the structure to take an extra amount of loading in comparison to the layered structure. This is mainly because of the sandwich configuration i.e. two stiff composite layers (face sheets) are separated by a thick low-density material layer (core). The fibrous composite materials have extensive advantages over their conventional counterparts and the requirement of overcoming the difficulties involved in the design of advanced high-speed flight vehicles. This, in turn, encouraged mainly to the usage of sandwich structural component instead of layer composite. Moreover, the requirement and usage of this sandwich configuration have become the priority due to the improvement and availability of the advanced fibre for the fabrication of the face sheet. In addition, the sandwich configuration has good bending rigidity, vibration characteristics, fatigue properties as well as low specific weight. However, the buckling is the major

issue need to be taken care during the designing of sandwich skins as wings of an aircraft. It is well known that the structural parts of high-speed aircraft are not only exposed to the aerodynamic loading only but also to the aerodynamic heating, which, further affects the whole structural stability. Due to this, the structure/structural components may buckle and the load-bearing capacity of the structure also deviates from the expected lines. This is severe for the structure which is working under either the individual and/or combination of loading i.e. under the influence of elevated temperature environment.

The structural responses (bending, vibration, buckling/post-buckling) of the laminated and sandwich composite plate are solved (Srinivas and Rao 1970, Singh *et al.* 1993, Striz *et al.* 1997, Hause *et al.* 1998, Thankam *et al.* 2003, Shiau and Kuo 2004, Girish and Ramachandra 2005) using different types of numerical (finite element/quadrature/meshfree/Galerkin) and benchmark (3-D elasticity) techniques to compute the temperature carrying capacity both the linear and nonlinear type strain. Similarly, the harmonic differential quadrature and discrete singular convolution algorithm have been adopted to investigate the static and dynamic characteristics of the isotropic/orthotropic composite circular/conical shell and plate structures by Civalek and his coworkers (2004, 2006, 2007a, b, 2008, 2011). Additionally, the structural model derived using the equivalent single layer theories to express the displacement function either by first-order and higher-order shear deformation theories (FSDT and HSDT) including von-Karman type nonlinear strain. Moreover, the HSDT type of kinematics is adopted by Matsunaga (2005,

*Corresponding author, Associate Professor
E-mail: pandask@nitrkl.ac.in

^aPh.D. Student
E-mail: pk.pankajkatariya@gmail.com

2006) to model and predict the buckling temperature values of the laminated and the sandwich plate structure. Similarly, the analytical technique (Zakeri and Alinia 2006) in association with the FSDT kinematics have been utilized to predict the buckling and the post-buckling temperature of the sandwich structures while exposed to the uniform thermal stresses. Likewise, the HSDT kinematics including the finite element method (FEM) have been adopted to compute the free vibration frequency (Garg *et al.* 2006) and the dynamic deflections (Park *et al.* 2008) of the skew sandwich plate, whereas the thermal buckling and post-buckling temperature are (Panda and Singh 2009) predicted for the laminated shell panel structure. The compressive strength of the laminated composite has been evaluated via experimentally to study the effect of the number of layers and the number of superposed delaminations (Amaro *et al.* 2014). Additionally, the classical laminate plate theory (CLPT) and the HSDT kinematic models are adopted in conjunction with von-Karman nonlinear strain to predict the finite element (FE) solutions for the eigenvalues i.e., frequency (Singh and Panda 2014), buckling (Juhazs and Szerkenyes 2015a, b) and post-buckling (Nikard and Asadi 2015) data of the layered composite structures with and without delamination. The deflection (Draiche *et al.* 2016) and buckling/post-buckling (Jun *et al.* 2016, Khayat *et al.* 2016) behaviour of the laminated composite flat/curved structures examined by considering the stretching effect using the FE steps in the framework of the FSDT and refined HSDT. In addition, the bending, buckling and free vibration (Abdelaziz *et al.* 2017) behaviour of the functionally graded (FG) beam/plate structure demonstrated by considering the stretching effect (Atmane *et al.* 2017, Bouhadra *et al.* 2018) via novel hyperbolic shear deformation theory. The thermal buckling behaviour of the laminated and FG structures are evaluated (Bellifa *et al.* 2017, Chikh *et al.* 2017, El-Haina *et al.* 2017; Fahsi *et al.* 2017, Menasria *et al.* 2017) by considering the stretching effect via refined HSDT and analytically. The structural responses (frequency, buckling) of the layered sandwich, FG and hybrid components are investigated (Zhai *et al.* 2018, Wu *et al.* 2018, Bourada *et al.* 2018, Kaci *et al.* 2018; Karami *et al.* 2018, Zine *et al.* 2018) using different robust techniques i.e., discrete singular convolution and differential quadrature, harmonic differential quadrature method in the framework of the FSDT and HSDT type of kinematics. In the recent past, the buckling responses of the stiffened plate are analysed by Sadamoto *et al.* (2017) and Yoshida *et al.* (2017) in the framework of the FSDT via the meshfree Galerkin flat-shell formulation in association with the reproducing kernel particle method. The structural member of sandwich materials possesses the excellent performance characteristic are under high-velocity impact loading during their operation in aerospace industry. The dynamic responses of these structures are analysed by Gao *et al.* (2018) performing set of experiments as well as the numerically solved via the ABAQUS/Explicit module. Further, the bending, buckling and the vibration responses of the nanobeam and the FG sandwich structures have been examined by Meksi *et al.* (2019), Bedia *et al.* (2019) using the nonlocal strain gradient theory by considering the

HSDT kinematics. Recently, the researchers (Draiche *et al.* 2019, Mahmoudi *et al.* 2019, Semmah *et al.* 2019) have studied the static, dynamic and stability characteristics of the laminated composite and FG, structures using a novel fractional nonlocal model in the framework of the FSDT and nonlocal higher-order strain gradient theories. A quasi 3D HSDT and the FSDT have been employed to examine the static, dynamic and stability characteristics of the layered, sandwich and FG structures on visco-Pasternak foundations (Addou *et al.* 2019, Zarga *et al.* 2019, Boukhelif *et al.* 2019, Boulefrakh *et al.* 2019, Boutaleb *et al.* 2019, Khiloun *et al.* 2019, Zaoui *et al.* 2019).

The review of earlier researches implied that the structural responses of the layered composite and sandwich components have been studied largely every now and then utilizing the established kinematic models and solution techniques with and without skew angle. However, it is important to note that the post-buckling temperature prediction of the skew sandwich analysis of the layered sandwich composite shell panel did not get much attention earlier. Also, the thermal post-buckling behaviour of the layered sandwich composite shell panel is different than the layered composite because of the dissimilar types of material of the face and core, which may behave otherwise than the expected line. Hence, considering all the above aspects, the current study aims where, ' t ' is the time, U_x , U_y and U_z are the displacement of any point within the panel along x , y and z directions, respectively. u_x^1 , u_y^1 and u_z^1 are the mid-plane displacement of any point within the panel along ξ_x , ξ_y , and ξ_z directions, respectively. Similarly, ψ_x^1 , ψ_y^1 and ψ_z^1 are the rotation of to understand the thermal post-buckling behaviour of the laminated sandwich composite shell panel including the tilted angle. In the present study, a generic nonlinear (Green-Lagrange strain) FE model is developed mathematically using the HSDT kinematics (maintain the parabolic distribution of the transverse shear stress) to count the deformation characteristics under the elevated temperature loading. The temperature load parameter of the sandwich structure is predicted in the post-buckled regime computationally through a home-made computer code developed in the MATLAB environment. The model accuracy is established by solving a few numerical problems as same as the earlier published examples including the consistency test. The verified model is extended to show the applicability by solving for the different geometrical and material parameters associated with the structural design.

2. Theory and general formulation

The sandwich structure is a special form of a layered structure having two thin stiff and strong laminated face sheets separated by a relatively thick and lightweight core material. Fig. 1 represents the geometry of the sandwich panel having a length " a ", width " b " and total thickness " h " is the combination of thicknesses of the face sheet " h_f " and the core " h_c ". The displacement model for the laminated sandwich shell panel is assumed to be (Singh and Panda

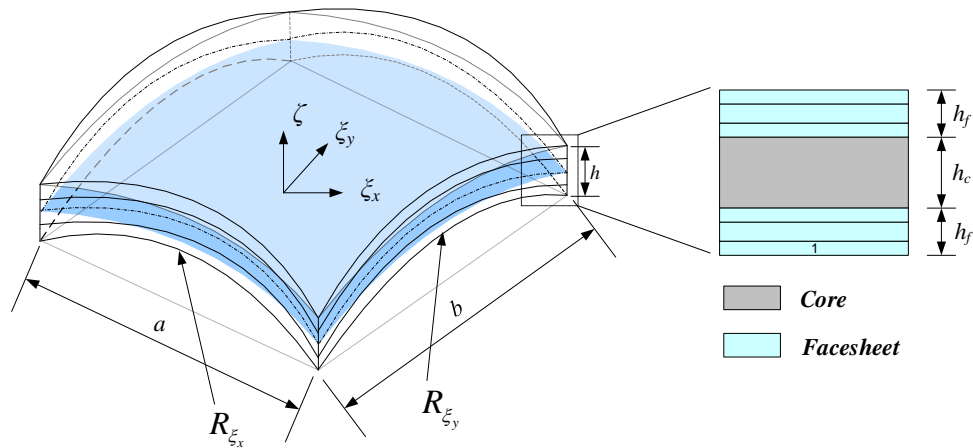


Fig. 1 Geometry and configuration of the sandwich panel

2014) higher-order including the stretching effect and given as

$$\left. \begin{aligned} U_x(\xi_x, \xi_y, \zeta, t) &= u_x^1(\xi_x, \xi_y, t) + \zeta \psi_x^1(\xi_x, \xi_y, t) + \zeta^2 \kappa_x^1(\xi_x, \xi_y, t) + \zeta^3 \lambda_x^1(\xi_x, \xi_y, t) \\ U_y(\xi_x, \xi_y, \zeta, t) &= u_y^1(\xi_x, \xi_y, t) + \zeta \psi_y^1(\xi_x, \xi_y, t) + \zeta^2 \kappa_y^1(\xi_x, \xi_y, t) + \zeta^3 \lambda_y^1(\xi_x, \xi_y, t) \\ U_z(\xi_x, \xi_y, \zeta, t) &= u_z^1(\xi_x, \xi_y, t) + \zeta \psi_z^1(\xi_x, \xi_y, t) \end{aligned} \right\} \quad (1)$$

normal to the mid-plane and extension terms, respectively along the corresponding directions. The higher-order functions in the equation i.e., κ_x^1 , κ_y^1 , λ_x^1 and λ_y^1 are defined from Taylor series expansion to express the desired mid-plane kinematics of the panel geometry.

The nonlinear strain-displacement relation based on Green-Lagrange type of nonlinearity as in Reddy (2004a) is adopted for the full geometric distortion of the sandwich composite shell panel and can be expressed as

where, the mid-plane linear $\{\epsilon_l\}$ and nonlinear $\{\epsilon_{nl}\}$ strain vector terms can be seen in Singh and panda (2014).

The constitutive relations for any arbitrary k^{th} layer in the sandwich composite panel accounting the external thermal environment has been elaborated as same as Reddy (2004b)

$$\begin{aligned} \{\epsilon\} &= \begin{Bmatrix} \epsilon_x \\ \epsilon_y \\ \epsilon_z \\ \gamma_{yz} \\ \gamma_{xz} \\ \gamma_{xy} \end{Bmatrix} = \begin{Bmatrix} \dot{U}_x + U_z/R_{\xi_x} \\ \dot{U}_y + U_z/R_{\xi_y} \\ \dot{U}_z \\ U_{y,z} + U_{z,y} - U_y/R_{\xi_y} \\ U_{x,z} + U_{z,x} - U_x/R_{\xi_x} \\ U_{x,y} + U_{y,x} + 2U_z/R_{\xi_x \xi_y} \end{Bmatrix} + \\ &\quad \left\{ \begin{aligned} &\left[\left(\dot{U}_x + U_z/R_{\xi_x} \right)^2 + \left(U_{y,x} + U_z/R_{\xi_x \xi_y} \right)^2 + \left(U_{z,x} - U_x/R_{\xi_x} \right)^2 \right] \\ &\left[\left(U_{x,y} + U_z/R_{\xi_x \xi_y} \right)^2 + \left(\dot{U}_y + U_z/R_{\xi_y} \right)^2 + \left(U_{z,y} \right)^2 \right] \\ &\frac{1}{2} \left[\left(U_{x,z} \right)^2 + \left(U_{y,z} \right)^2 + \left(\dot{U}_z \right)^2 \right] \\ &2 \left[\left(U_{x,y} \right) \left(\dot{U}_x + U_z/R_{\xi_x} \right) + \left(U_{y,z} \right) \left(\dot{U}_y + U_z/R_{\xi_y} \right) + \left(\dot{U}_z \right) \left(U_{z,y} - U_y/R_{\xi_y} \right) \right] \\ &2 \left[\left(U_{x,z} \right) \left(\dot{U}_x + U_z/R_{\xi_x} \right) + \left(U_{y,z} \right) \left(U_{y,x} + U_z/R_{\xi_x \xi_y} \right) + \left(\dot{U}_z \right) \left(U_{z,x} - U_x/R_{\xi_x} \right) \right] \\ &2 \left[\left(U_{x,y} + U_z/R_{\xi_x \xi_y} \right) \left(\dot{U}_x + U_z/R_{\xi_x} \right) + \left(\dot{U}_y + U_z/R_{\xi_y} \right) \left(U_{y,x} + U_z/R_{\xi_x \xi_y} \right) + \left(U_{z,y} - U_y/R_{\xi_y} \right) \left(U_{z,x} - U_x/R_{\xi_x} \right) \right] \end{aligned} \right\} \quad (2) \\ \text{or } \{\epsilon\} &= \{\epsilon_l\} + \{\epsilon_{nl}\} \end{aligned}$$

$$\{\sigma\}^k = [\bar{Q}]^k \left[\{\varepsilon\}^k - \{\alpha\}^k \Delta T \right] \quad (3)$$

From the constitutive expression (Eq. (3)), the required stress and the strain tensors can be presented in the expanded form i.e.,

$$\{\sigma\}^k = \begin{Bmatrix} \sigma_x & \sigma_y & \sigma_z & \tau_{yz} & \tau_{xz} & \tau_{xy} \end{Bmatrix}^T \quad \text{and} \quad \{\varepsilon\}^k = \begin{Bmatrix} \varepsilon_x & \varepsilon_y & \varepsilon_z & \gamma_{yz} & \gamma_{xz} & \gamma_{xy} \end{Bmatrix}^T. \quad \text{Also, } [\bar{Q}]^k \text{ is the transformed reduced stiffness matrix, whereas, the uniform temperature rise is } \Delta T. \text{ Similarly, the transformed linear thermal expansion coefficient vector of the } k^{\text{th}} \text{ layer represented in the equation as}$$

$$\{\alpha\}^k = \begin{Bmatrix} \alpha_x & \alpha_y & \alpha_{xy} \end{Bmatrix}^T$$

Now, to obtain the required in-plane temperature forces are computed by integrating the Eq. (3) over the thickness of the panel and defined as in the following lines.

$$\begin{Bmatrix} \{N_{\Delta T}\} \\ \{M_{\Delta T}\} \\ \{P_{\Delta T}\} \end{Bmatrix} = \sum_{k=1}^N \int_{\zeta_{k-1}}^{\zeta_k} [\bar{Q}]^k \begin{Bmatrix} \alpha_x \\ \alpha_y \\ 2\alpha_{xy} \end{Bmatrix}^k (1, \zeta, \zeta^2) \Delta T d\zeta \quad (4)$$

where, $\{N_{\Delta T}\}$, $\{M_{\Delta T}\}$ and $\{P_{\Delta T}\}$ are the resultant compressive in-plane membrane force vectors, moments and the higher-order terms, respectively.

Now, the strain energy ($U_{S.E.}$) of the sandwich composite shell panel can be expressed as

$$U_{S.E.} = \frac{1}{2} \int_V \{\varepsilon\}_i^T \{\sigma_i\} dV \quad (5)$$

The final form of the energy functional of the sandwich panel under uniform temperature loading is obtained by replacing the total strain and the stress tensors from the Eqs. (2) and (3) into the above Eq. (5) and can be written as

$$U_{S.E.} = \frac{1}{2} \int_V \{\varepsilon_i\}_i^k \left[[\bar{Q}]^k \left(\{\varepsilon_i\}_i^k - \{\alpha\}_i^k \Delta T \right) \right] dV \quad (6)$$

Now, the total work done ($W_{\Delta T}$) by the in-plane thermal force ($\{N_{\Delta T}\}$, $\{N_{\Delta y}\}$ and $\{N_{\Delta xy}\}$) due to the influence of the uniform temperature rise (ΔT) of the curved sandwich composite panel is computed using Green-Lagrange type of strain field and written as

$$W_{\Delta T} = \frac{1}{2} \int_V \left[\begin{aligned} & \left[(\dot{U}_x)^2 + (U_{y,x})^2 + (U_{z,x})^2 \right] \{N_{\Delta T}\} + \\ & \left[(U_{x,y})^2 + (\dot{U}_y)^2 + (U_{z,y})^2 \right] \{N_{\Delta y}\} + \\ & 2 \left[(\dot{U}_x)(U_{x,y}) + (U_{y,x}) \right] \{N_{\Delta xy}\} \\ & \left[(\dot{U}_y) + (U_{z,x})(U_{z,y}) \right] \end{aligned} \right] dV \quad (7)$$

The above work done expression is linearized by employing the procedure as given in Cook et al. (2009) and conceded as

$$W_{\Delta T} = \frac{1}{2} \int_A \{\varepsilon_G\}^T [D_G] \{\varepsilon_G\} dA \quad (8)$$

where, $\{\varepsilon_G\}$ and $[D_G]$ represents the geometric strain and the material property matrix, respectively due to the in-plane thermal loading.

In the current study, a nine-noded curved isoparametric element with ten unknowns per node $u_x^1, u_y^1, u_z^1, \psi_x^1, \psi_y^1, \psi_z^1, \kappa_x^1, \kappa_y^1, \lambda_x^1$ and λ_y^1 is used to develop the finite element procedure. The generalized displacements fields included in the present study in terms of nodal variables can be expressed as

$$\begin{aligned} u_x^1 &= \sum_{i=1}^9 N_i u_{xi}^1, u_y^1 = \sum_{i=1}^9 N_i u_{yi}^1, u_z^1 = \sum_{i=1}^9 N_i u_{zi}^1, \\ \psi_x^1 &= \sum_{i=1}^9 N_i \psi_{xi}^1, \psi_y^1 = \sum_{i=1}^9 N_i \psi_{yi}^1, \psi_z^1 = \sum_{i=1}^9 N_i \psi_{zi}^1, \\ \kappa_x^1 &= \sum_{i=1}^9 N_i \kappa_{xi}^1, \kappa_y^1 = \sum_{i=1}^9 N_i \kappa_{yi}^1, \lambda_x^1 = \sum_{i=1}^9 N_i \lambda_{xi}^1, \\ \lambda_y^1 &= \sum_{i=1}^9 N_i \lambda_{yi}^1, \end{aligned} \quad (9)$$

In addition, the displacement vector $\{\delta\}$ at any point on the mid-surface can be expressed as follows

$$\{\delta\} = N_i \{\delta_i\} \quad (10)$$

where, $\{\delta_i\} = [u_{xi}^1, u_{yi}^1, u_{zi}^1, \psi_{xi}^1, \psi_{yi}^1, \psi_{zi}^1, \kappa_{xi}^1, \kappa_{yi}^1, \lambda_{xi}^1, \lambda_{yi}^1]^T$ is the nodal displacement vector of the model and N_i is the interpolating function associated with node 'i'.

Now, substituting the Eq. (10) into the Eqs. (6) and (8), the corresponding functionals i.e. the strain energy and the work done expressions are modified as

$$U_{S.E.} = \frac{1}{2} \int_A \begin{Bmatrix} \{\bar{\varepsilon}_l\}^T [D_1] \{\bar{\varepsilon}_l\} + \\ \{\bar{\varepsilon}_l\}^T [D_2] \{\bar{\varepsilon}_{nl}\} + \\ \{\bar{\varepsilon}_{nl}\}^T [D_3] \{\bar{\varepsilon}_l\} + \\ \{\bar{\varepsilon}_{nl}\}^T [D_4] \{\bar{\varepsilon}_{nl}\} \end{Bmatrix} dA - \{F_{\Delta T}\}_i \quad (11)$$

$$W_{\Delta T} = \frac{1}{2} \int_A \{\delta\}_i^T [B_G]_i^T [D_G] [B_G]_i \{\delta\}_i dA \quad (12)$$

where,

$$\begin{aligned} [D_1] &= \int_{-h/2}^{+h/2} [T^l]^T [Q] [T^l] dz, [D_2] = \int_{-h/2}^{+h/2} [T^l]^T [Q] [T^{nl}] dz, \\ [D_3] &= \int_{-h/2}^{+h/2} [T^{nl}]^T [Q] [T^l] dz, [D_4] = \int_{-h/2}^{+h/2} [T^{nl}]^T [Q] [T^{nl}] dz \end{aligned}$$

Similarly, the linear and nonlinear mid-plane strain vectors are rewritten in the form of the nodal displacement vectors and can be expressed as

$$\{\bar{\epsilon}_l\} = [B]\{\delta\}, \{\bar{\epsilon}_{nl}\} = [A][G]\{\delta\} \quad (13)$$

where, $[B]$ is the linear strain-displacement matrix defined with the help of nodal shape functions and operator matrix. Similarly, $[G]$ associated with nonlinear mid-plane strain as same as the linear case whereas components of $[A]$ are the function of displacements. The details regarding the individual matrices can be seen in Singh and Panda (2014).

Now, by minimizing the energy expression, the final form of the governing equation for the sandwich composite shell panel is obtained and expressed as

$$\delta \Pi = 0 \quad (14)$$

where, $\Pi = (U_{S.E.} - W_{\Delta T})$.

Finally, by using the Eqs. (6)-(14), the final governing equilibrium equation of the sandwich structural system can be expressed as Panda and Singh (2009)

$$\begin{aligned} ([K_l] + [K_{nl}(\delta)])\{\delta\} &= \{F_{\Delta T}\} \\ \text{or, } ([K_l] + [K_{nl}]) + T_{cr} [K_G] \{\delta\} &= 0 \end{aligned} \quad (15)$$

The equation consist of terms $\{\delta\}$, $[K_l]$ and $[K_{nl}]$ are the global displacement vector, the linear global stiffness matrix and the nonlinear global stiffness matrix, respectively. Also, the thermal force vector seen in the system equation due to the elevated environment has been dropped and the corresponding effect included in the system via geometrical stiffness i.e., $[K_G]$ in the further steps (Thankam *et al.* 2003). The inclusion of the geometrical stiffness matrix technique is mainly adopted to make the equation a nonlinear eigenvalue type. Now, the linear and nonlinear eigenvalues are computed by solving the Eq. (15) and the steps followed (Panda and Singh 2009) can be seen below. Now, the minimum eigenvalue predicted is the critical buckling temperature load and denoted as T_{cr} .

- The geometry and material parameters are initialized as a first step.
- The relevant structural elemental matrices are evaluated using the finite element technique.
- The final/global form of each case achieved further using the FE methodology.
- Now, to avoid the rigid body motion, the edge support conditions are applied and the final governing equation is solved using the direct iterative technique.
- First, the linear response (critical buckling temperature parameter) is achieved at the first step of iteration process.
- Further, the iteration process has been extended to obtain the nonlinear responses (post-buckling temperature parameter).

The iterations will continue until the two consecutive values converge, considering the necessary criteria.

3. Results and discussions

The post-buckling behaviour of the laminated composite plate is examined using the presently developed numerical model. The critical buckling temperature data are presented

in the non-dimensional form using the formula: $\Omega_T = \alpha_T T_{cr} (b/h)^2$. The material properties considered for the present numerical analysis are taken as same as Thankam *et al.* (2003) and provided below for the sake of clarity. The computation of the responses are obtained using different sets of end support conditions and the details of end boundaries can be seen in Table 1.

$$\begin{aligned} E_{\xi_x} / E_{\xi_y} &= 40; G_{\xi_x \xi_y} / E_{\xi_y} = 0.60; G_{\xi_x \xi_z} = G_{\xi_x \xi_y}; \\ G_{\xi_y \xi_z} / E_{\xi_y} &= 0.50; \nu_{\xi_x \xi_y} = 0.25; \alpha_{\xi_y} / \alpha_{\xi_x} = 10 \end{aligned}$$

The model verification is one of the major steps in every numerical analysis, hence, the current nonlinear FE model consistency has been checked for different numbers of elements i.e., coarse to fine mesh effect on the desired output. It is important to mention that the results are verified for the laminated composite plate structure instead of the sandwich component due to the unavailability of thermal post-buckling case of flat/curved sandwich. The model validity has been established based on the assumption of negligible core layer thickness with infinite radii, which, in turn, implies as laminated composite flat structure. Moreover, the flat panels are the simplest form of curved geometry. Table 2 presented the temperature ratio of the nonlinear (T) to the critical buckling (T_{cr}) values for different element sizes including the reference data. The results are calculated using the same material and the dimensional values for the sake of comparison. The difference between the ratios is due to the types of mid-plane kinematics and nonlinear strain displacement relations. The current model utilizes the higher-order mid-plane kinematics and Green-Lagrange strain with stretching term effect whereas the reference model adopted von-Karman nonlinearity in the framework of the FSDT. The FE convergence indicates the model solidity for the current analysis and 36 elements has been utilized to compute the new post-buckling data.

3.1 Parametric study

Now, several examples are solved to show the influences of various geometrical parameters (amplitude ratio, W_{max}/h ; length-to-width ratio, a/b ; side-to-thickness ratio, b/h ; curvature ratio, R/a ; core-to-face thickness ratio, h_c/h_f) on the nonlinear buckling load parameter of skew ($\phi = 0^\circ, 15^\circ, 30^\circ$ and 45°) sandwich ($0^\circ/90^\circ/\text{Core}/90^\circ/0^\circ$) shell panels.

Table 1 End support conditions

| End conditions | At edge $\xi_x = 0, a$ | At edge $\xi_y = 0, b$ |
|----------------|---|---|
| Simply-support | $U_y = U_z = \psi_y = \psi_z = \kappa_y = \zeta_y = 0$ | $U_x = U_z = \psi_x = \psi_z = \kappa_x = \zeta_x = 0$ |
| Clamped | $U_x = U_y = U_z = \psi_x = \psi_y = \psi_z = \kappa_x = \kappa_y = \kappa_z = \zeta_x = \zeta_y = 0$ | $U_x = U_y = U_z = \psi_x = \psi_y = \psi_z = \kappa_x = \kappa_y = \kappa_z = \zeta_x = \zeta_y = 0$ |

Table 2 Convergence and validation of the post-buckling ratio (T/T_{cr}) for hinged square ($45^\circ/45^\circ$)_s laminated composite plate ($b/h = 100$)

| Number of elements | T/T_{cr} | | | | |
|------------------------------|---------------------------------|--------|--------|--------|--------|
| | Amplitude ratio (W_{max}/h) | | | | |
| | 0.2 | 0.4 | 0.6 | 0.8 | 1.0 |
| 4 | 1.0079 | 1.0312 | 1.0697 | 1.1225 | 1.1896 |
| 9 | 1.0068 | 1.0269 | 1.0604 | 1.1066 | 1.1646 |
| 16 | 1.0076 | 1.0307 | 1.0687 | 1.1214 | 1.1882 |
| 25 | 1.0091 | 1.0342 | 1.0794 | 1.1408 | 1.2192 |
| 36 | 1.0102 | 1.0412 | 1.0925 | 1.1619 | 1.2551 |
| 49 | 1.0114 | 1.0475 | 1.1052 | 1.1871 | 1.2915 |
| 64 | 1.0136 | 1.0545 | 1.1206 | 1.2142 | 1.3351 |
| Singh <i>et al.</i> (1993) | 1.051 | 1.204 | 1.459 | 1.322 | 1.371 |
| Thankam <i>et al.</i> (2003) | 1.051 | 1.203 | 1.459 | 1.318 | 1.366 |

The material properties of each example of the laminated sandwich shell structures are taken from Matsunaga (2005) and provided in the following lines:

Face (graphite/epoxy)

$$E_{\xi_x} = 2 \times 10^5 \text{ MPa}; E_{\xi_y} = 8 \times 10^3 \text{ MPa}; G_{\xi_x \xi_y} = 2.2 \times 10^3 \text{ MPa};$$

$$G_{\xi_x \xi_y} = G_{\xi_y \xi_x} = 5 \times 10^3 \text{ MPa}; \nu_{\xi_x \xi_y} = 0.35; \nu_{\xi_y \xi_x} = \nu_{\xi_x \xi_z} = 0.25;$$

$$\alpha_{\xi_x} = -2\alpha_0; \alpha_{\xi_y} = 50\alpha_0; \alpha_0 = 1 \times 10^{-6} / K$$

Core (soft)

$$E_{\xi_x} = 1000 \text{ MPa}; E_{\xi_y} = 2 \times 10^3 \text{ MPa}; G_{\xi_x \xi_y} = G_{\xi_y \xi_x} = 800 \text{ MPa};$$

$$G_{\xi_y \xi_z} = 3700 \text{ MPa}; \nu_{\xi_x \xi_y} = \nu_{\xi_x \xi_z} = 0.25; \nu_{\xi_y \xi_z} = 0.35;$$

$$\alpha_{\xi_x} = \alpha_{\xi_y} = 30\alpha_0; \alpha_0 = 1 \times 10^{-6} / K$$

3.1.1 Influence of the side-to-thickness ratio

The first numerical problem is solved to predict the post-buckling behaviour of a square simply supported skew panel of two different geometrical configurations i.e., cylindrical (one of the radius is infinite) and spherical (both radii of curvature are equal) (refer to Fig. 2). The responses are plotted for five different thickness ratios ($b/h = 5, 15, 25, 50$, and 100) including the other associated data i.e. $W_{max}/h = 0.4$; $R/a = 10$; and $h_c/h_f = 5$. It is well-known that the variation in the structural stiffness affects the responses significantly which can be seen in the figure i.e., the buckling load parameter increases with an increase in b/h and ϕ . Also, from the results it can be noticed that the spherical geometry has higher temperature carrying capacity in comparison to the cylinder.

3.1.2 Influence of curvature ratio

The current example also reported for two different geometrical configurations having equal (spherical) and unequal (hyperboloid) curvatures. The importance of curvature values on the temperature data in the post-buckling regime have been obtained and presented in Fig. 3.

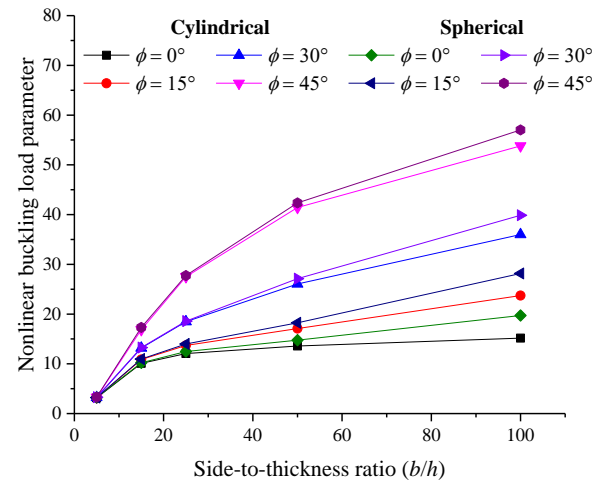


Fig. 2 Effect of the side-to-thickness ratios on the nonlinear buckling load parameter of a skew sandwich cylindrical and spherical shell panel

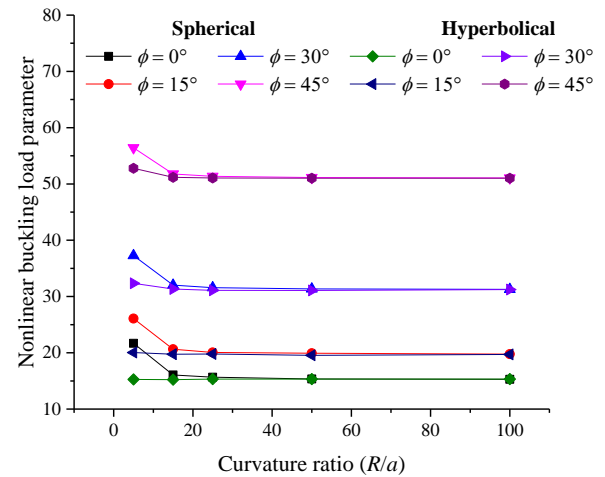


Fig. 3 Effect of the curvature ratios on the nonlinear buckling load parameter of a skew sandwich spherical and hyperbolical shell panel

The numerical problem has been solved for the thin ($b/h = 50$) square clamped skew sandwich ($h_c/h_f = 10$) panel of five curvature ratios ($R/a = 5, 15, 25, 50$ and 100) by setting the amplitude as: $W_{max}/h = 0.6$. The responses follow a similar line for the skew angle as in the earlier example i.e., the buckling load parameters are increasing when the skew angle increases. But, the buckling load parameter value follows a declining trend with the increase of R/a . This is because of fact that the panel becomes flat while R/a increases, whereas the spherical geometry shows higher strength in comparison to the hyperbolical shell panel.

3.1.3 Influence of length-to-width ratio

The nonlinear buckling load parameters are obtained by varying the length-to-width ratio of a square clamped skew

cylindrical and elliptical sandwich shell panel and presented in Table 3. The results are computed by considering the geometrical parameters as, $a/b = 1, 1.5, 2, 2.5$, and 3 ; $b/h = 10$; $R/a = 10$; $h_c/h_f = 10$; and $W_{max}/h = 0.4$. It is understood from the earlier example that the nonlinear buckling load parameter value increases as the skew angle increase and the same type of trend have been observed in this example too. The results also point out that the nonlinear buckling load parameter values are following a declining type of trend with the increase in the values of a/b . In addition, the elliptical shell geometry has a higher nonlinear buckling load parameter values in comparison with the cylindrical shell geometry.

3.1.4 Influence of amplitude ratio

In the previous set of numerical examples influence of b/h , R/a , and a/b with the skew angles are investigated. Now, the responses are computed to examine the effect of the amplitude ratios on a square simply supported cylindrical and spherical skew sandwich shell panel can be seen in Fig. 4. For the computation purpose, the geometrical data has been considered as: $W_{max}/h = 0.2, 0.4, 0.6, 0.8$, and 1.0 ; $b/h = 100$; $R/a = 10$; and $h_c/h_f = 5$. The effect of the skew angle is similar as discussed in the earlier cases i.e., the nonlinear buckling load parameter values increase with an increase in the skew angles. In addition, the nonlinear buckling load parameter values follow an increasing type of trend with an increase in the amplitude ratios. Further, the spherical shell geometry shows higher values compared to the cylindrical shell geometry.

3.1.4 Influence of amplitude ratio

In the previous set of numerical examples influence of b/h , R/a , and a/b with the skew angles are investigated. Now, the responses are computed to examine the effect of the amplitude ratios on a square simply supported cylindrical and spherical skew sandwich shell panel can be seen in Fig. 4.

Table 3 Effect of the length-to-width ratios on the nonlinear buckling load parameter of a skew sandwich cylindrical and elliptical shell panel

| a/b | Shell geometry | Skew angle (ϕ) | | | |
|-------|----------------|-----------------------|------------|------------|------------|
| | | 0° | 15° | 30° | 45° |
| 1.0 | Cylindrical | 18.8299 | 18.9901 | 19.5021 | 20.4281 |
| 1.5 | | 13.1437 | 13.1939 | 13.1966 | 16.1487 |
| 2.0 | | 9.4574 | 9.6972 | 10.6103 | 12.494 |
| 2.5 | | 6.9678 | 7.1551 | 7.9648 | 9.7531 |
| 3.0 | | 5.2811 | 5.4643 | 6.1333 | 7.7301 |
| 1.0 | Elliptical | 18.9110 | 19.0832 | 19.5780 | 20.4828 |
| 1.5 | | 13.4361 | 13.6882 | 14.5215 | 16.2273 |
| 2.0 | | 9.5790 | 9.8319 | 10.7051 | 12.5765 |
| 2.5 | | 7.0158 | 7.2283 | 8.0401 | 9.8271 |
| 3.0 | | 5.3510 | 5.5165 | 6.2035 | 7.8034 |

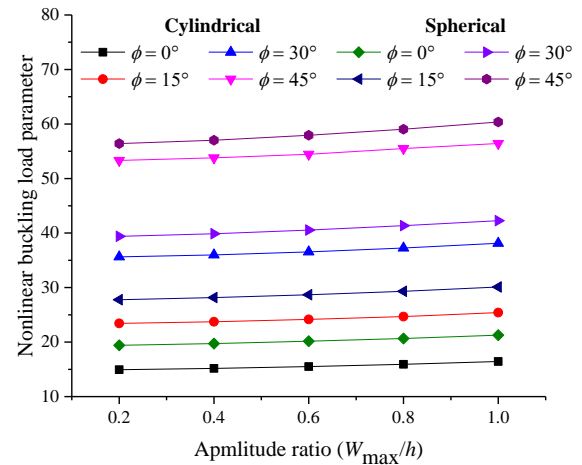


Fig. 4 Effect of the amplitude ratios on the nonlinear buckling load parameter of a skew sandwich cylindrical and spherical shell panel

For the computation purpose, the geometrical data has been considered as: $W_{max}/h = 0.2, 0.4, 0.6, 0.8$, and 1.0 ; $b/h = 100$; $R/a = 10$; and $h_c/h_f = 5$. The effect of the skew angle is similar as discussed in the earlier cases i.e., the nonlinear buckling load parameter values increase with an increase in the skew angles. In addition, the nonlinear buckling load parameter values follow an increasing type of trend with an increase in the amplitude ratios. Further, the spherical shell geometry shows higher values compared to the cylindrical shell geometry.

3.1.5 Influence of core-to-face thickness ratio

In this example, the influence of the core-to-face thickness ratio ($h_c/h_f = 5, 10, 15, 20$ and 25) on the nonlinear buckling load parameter of a square simply supported hyperbolic and elliptical skew sandwich shell panel are analysed and presented in Fig. 5. For the computation purpose, the geometrical parameters are considered as: $b/h = 50$; $R/a = 5$; $W_{max}/h = 0.2$. The results show that an increase in the core-to-face thickness ratios values tends to increase the nonlinear buckling load parameter values. In addition, the skew angle has also a substantial effect on the responses. Further, the elliptical shell geometry has a higher nonlinear buckling load parameter values in comparison with the hyperbolic shell geometry.

3.1.6 Different shell panel geometry

Finally, a numerical example is solved to check the behaviour of all different shell panels (flat panel, cylindrical, spherical, hyperbolic, and elliptical) on nonlinear buckling load parameter as shown in Fig. 6. In this case, a square simply supported skew sandwich shell panels has been considered with other important geometrical parameters are $b/h = 10$; $R/a = 5$; $W_{max}/h = 0.2$; and $h_c/h_f = 5$. The results are obtained for various skew angles and the effect of the same has been discussed earlier.

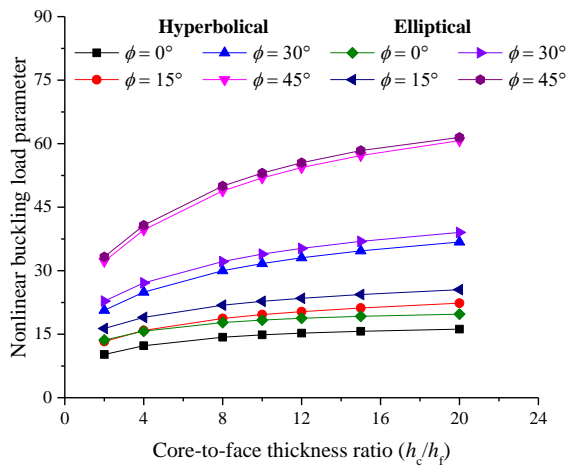


Fig. 5 Effect of the core-to-face thickness ratios on the nonlinear buckling load parameter of a skew sandwich Hyperbolic and elliptical shell panel

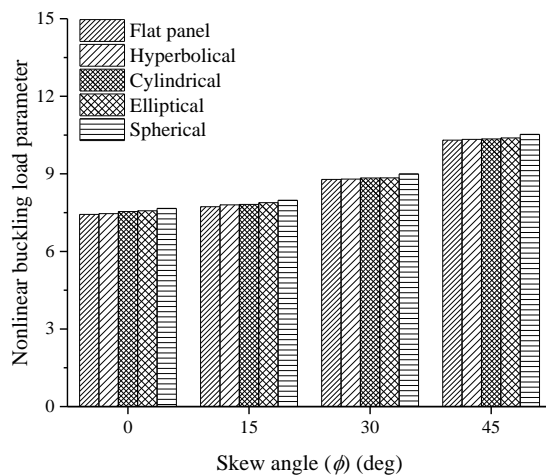


Fig. 6 Nonlinear buckling load parameter responses of the different sandwich skew shell panel

It is noticed from the responses that the spherical shell geometry has the higher nonlinear buckling load parameter value compared to other shell geometries and it follows declining type of trend i.e., spherical to elliptical, cylindrical, hyperbolic and flat panel.

4. Conclusions

The temperature load-carrying capacity of low-density core type sandwich structural component is investigated numerically via a higher-order FE model in the framework of equivalent single layer theory. The mathematical model is derived using the full nonlinear strain kinematics i.e. Green-Lagrange strain to accumulate the geometrical

distortion under the elevated thermal field in the post-buckling regime. The temperature data are obtained computationally with the help of a nonlinear FE code prepared in MATLAB including the direct iterative method. Additionally, the model includes all of the nonlinear strain terms to investigate the exact geometrical distortion. The FE model consistency and accuracy has been established as a priori for the subsequent implementation to compute the required temperature load parameter in the post-buckling regime. The model is induced further to solve different kind of numerical examples after the necessary verification. The examples have been covered the various aspects of the sandwich composite shell panels and the comprehensive understanding from the parametric study are listed in the following lines.

- The model accuracy and capability have been sought clearly from the corresponding convergence and the comparison study.
- In general, the critical temperature parameter in the post-buckling regime of the sandwich shell structure is increasing while the side-to-thickness ratio, the amplitude ratio, the core-to-face thickness ratio and the skew angle increases. However, the temperature value decreases when the curvature ratio and the length-to-width ratio of the shell panel increases. This is because of the alteration of structural stiffness due to the change in the geometrical parameter.
- Also, it can be implied from the responses that the spherical shell geometry has the higher nonlinear buckling load parameter values in comparison to each kind of shell configurations (due to two equal curvature along its principal material direction).

References

- Abdelaziz, H.H., Meziane, M.A.A, Bousahla, A.A., Tounsi, A., Mahmoud, S.R. and Alwabli, A.S. (2017), "An efficient hyperbolic shear deformation theory for bending, buckling and free vibration of FGM sandwich plates with various boundary conditions", *Steel Compos. Struct.*, **25**(6), 693-704. <https://doi.org/10.12989/scs.2017.25.6.693>.
- Addou, F.Y., Meradjah, M., Bousahla, A.A., Benachour, A., Bourada, F., Tounsi, A. and Mahmoud, S.R. (2019), "Influences of porosity on dynamic response of FG plates resting on Winkler/Pasternak/Kerr foundation using quasi 3D HSDT", *Comput. Concrete*, **24**(4), 347-367. <https://doi.org/10.12989/cac.2019.24.4.347>.
- Akgöz, B. and Civalek, O. (2011), "Nonlinear vibration analysis of laminated plates resting on nonlinear two-parameters elastic foundations", *Steel Compos. Struct.*, **11**(5), 403-421. <https://doi.org/10.12989/scs.2011.11.5.403>.
- Amaro, A.M., Reis, P.N.B., de Moura, M.F.S.F. and Neto, M.A. (2014), "Buckling analysis of laminated composite plates submitted to compression after impact", *Fibers Polym.*, **15**(3), 560-568. <https://doi.org/10.1007/s12221-014-0560-x>.
- Atmane, H.A., Tounsi, A. Bernard, F. (2017), "Effect of thickness stretching and porosity on mechanical response of a functionally graded beams resting on elastic foundations", *Int. J. Mech. Mater. Des.*, **13**(1), 71-84. <https://doi.org/10.1007/s10999-015-9318-x>.

- Bedia, W.A., Houari, M.S.A., Bessaim, A., Bousahla, A.A., Tounsi, A., Saeed, T. and Alhodaly, M.S. (2019), "A new hyperbolic two-unknown beam model for bending and buckling analysis of a nonlocal strain gradient nanobeams", *J. Nano Res.*, **57**, 175-191. <https://doi.org/10.4028/www.scientific.net/JNanoR.57.175>.
- Bellifa, H., Bakora, A., Tounsi, A., Bousahla, A.A. and Mahmoud, S.R. (2017), "An efficient and simple four variable refined plate theory for buckling analysis of functionally graded plates", *Steel Compos. Struct.*, **25**(3), 257-270. <https://doi.org/10.12989/scs.2017.25.3.257>.
- Bouhadra, A., Tounsi, A., Bousahla, A.A., Benyoucef, S. and Samy R. (2018), "Improved HSDT accounting for effect of thickness stretching in advanced composite plates", *Struct. Eng. Mech.*, **66**(1), 61-73. <https://doi.org/10.12989/sem.2018.66.1.061>.
- Boukhelif, Z., Bouremana, M., Bourada, F., Bousahla, A.A., Bourada, M., Tounsi, A. and Al-Osta, M.A. (2019), "A simple quasi-3D HSDT for the dynamics analysis of FG thick plate on elastic foundation", *Steel Compos. Struct.*, **31**(5), 503-516. <https://doi.org/10.12989/scs.2019.31.5.503>.
- Boulefrakh, L., Hebali, H., Chikh, A., Bousahla, A.A., Tounsi, A. and Mahmoud, S.R. (2019), "The effect of parameters of visco-Pasternak foundation on the bending and vibration properties of a thick FG plate", *Geomech. Eng.*, **18**(2), 161-178. <https://doi.org/10.12989/gae.2019.18.2.161>.
- Bourada, F., Amara, K., Bousahla, A.A., Tounsi, A. and Mahmoud, S.R. (2018), "A novel refined plate theory for stability analysis of hybrid and symmetric S-FGM plates", *Struct. Eng. Mech.*, **68**(6), 661-675. <https://doi.org/10.12989/sem.2018.68.6.661>.
- Boutaleb, S., Benrahou, K.H., Bakora, A., Algarni, A., Bousahla, A.A., Tounsi, A., Tounsi A., and Mahmoud, S.R. (2019), "Dynamic Analysis of nanosize FG rectangular plates based on simple nonlocal quasi 3D HSDT", *Adv. Nano Res.*, **7**(3), 189-206. <https://doi.org/10.12989/anr.2019.7.3.191>.
- Chikh, A., Tounsi, A., Hebali, H. and Mahmoud, S.R. (2017), "Thermal buckling analysis of cross-ply laminated plates using a simplified HSDT", *Smart Struct. Syst.*, **19**(3), 289-297. <https://doi.org/10.12989/sss.2017.19.3.289>.
- Civalek, O. (2006), "Free vibration analysis of composite conical shells using the discrete singular convolution algorithm", *Steel Compos. Struct.*, **6**(4), 353-366. <https://doi.org/10.12989/scs.2006.6.4.353>.
- Civalek, O. (2007a) "Linear vibration analysis of isotropic conical shells by discrete singular convolution (DSC)", *Struct. Eng. Mech.*, **25**(1), 127-130. <https://doi.org/10.12989/sem.2007.25.1.127>.
- Civalek, O. (2008), "Vibration analysis of conical panels using the method of discrete singular convolution", *Commun. Numer. Meth. Eng.*, **24**, 169-181. <https://doi.org/10.1002/cnm.961>.
- Civalek, O. and Acar, M.H. (2007b), "Discrete singular convolution method for the analysis of Mindlin plates on elastic foundations", *Int. J. Press. Vessels Pip.*, **84**(9), 527-535. <https://doi.org/10.1016/j.ijpvp.2007.07.001>.
- Civalek, O. and Ulker, M. (2004), "Harmonic differential quadrature (HDQ) for axisymmetric bending analysis of thin isotropic circular plates", *Struct Eng. Mech.*, **17**(1), 1-14. <https://doi.org/10.12989/sem.2004.17.1.001>.
- Cook, R.D., Malkus, D.S., Plesha, M.E. and Witt, R.J. (2009), *Concepts and Applications of Finite Element Analysis*, 4th edition, John Wiley & Sons Pvt. Ltd., Singapore.
- Draiche, K., Bousahla, A.A., Tounsi, A., Alwabli, A.S., Tounsi, A. and Mahmoud, S.R. (2019), "Static analysis of laminated reinforced composite plates using a simple first-order shear deformation theory", *Comput. Concrete*, **24**(4), 369-378. <https://doi.org/10.12989/cac.2019.24.4.369>.
- Draiche, K., Tounsi A. and Mahmoud, S.R. (2016), "A refined theory with stretching effect for the flexure analysis of laminated composite plates", *Geomech. Eng.*, **11**(5), 671-690. <https://doi.org/10.12989/gae.2016.11.5.671>.
- El-Haina, F., Bakora, A., Bousahla, A.A., Tounsi, A. and Mahmoud, S.R. (2017), "A simple analytical approach for thermal buckling of thick functionally graded sandwich plates", *Struct. Eng. Mech.*, **63**(5), 585-595. <https://doi.org/10.12989/sem.2017.63.5.585>.
- Fahsi, A., Tounsi, A., Hebali, H., Chikh, A., Adda Bedia, E.A. and Mahmoud, S.R. (2017), "A four-variable refined nth-order shear deformation theory for mechanical and thermal buckling analysis of functionally graded plates", *Geomech. Eng.*, **13**(3), 385-410. <https://doi.org/10.12989/gae.2017.13.3.385>.
- Gao, G.W., Tang, E.L., Feng, M.H., Han, Y.F., Li, Y., Liu, M., Xu, Y.L., Wang, L., Lin, X.C., Wang, R.Z., Cheng, Y.G., Zhao, L.L., Liang, Z.G., Wang, J.R., Zhao, G.J., Gao, Q. and Zheng, T.Z. (2018), "Research on dynamic response characteristics of CFRP/Al HC SPs subjected to high-velocity impact", *Def. Technol.*, **14**(5), 503-512. <https://doi.org/10.1016/j.dt.2018.06.017>.
- Garg, A.K., Khare, R.K. and Kant, T. (2006), "Free vibration of skew fiber-reinforced composite and sandwich laminates using a shear deformable finite element model", *J Sand. Struct Mater.*, **8**(1), 33-53. <https://doi.org/10.1177/1099636206056457>.
- Girish, J. and Ramachandra, L.S. (2005), "Postbuckling and vibration analysis of Antisymmetric angle-ply composite plates", *J. Therm. Stresses*, **28**(11), 1145-1159. <https://doi.org/10.1080/014957390967866>.
- Hause, T., Librescu, L. and Camarda, C.J. (1998), "Postbuckling of anisotropic flat and doubly-curved sandwich panels under complex loading conditions", *Int. J. Solids Struct.*, **35**(23), 3007-3027. [https://doi.org/10.1016/S0020-7683\(97\)00360-0](https://doi.org/10.1016/S0020-7683(97)00360-0).
- Juhász, Z. and Szekrényes, A. (2015a), "Progressive buckling of a simply supported delaminated orthotropic rectangular composite plate", *Int. J. Solids Struct.*, **69-70**, 217-229. <https://doi.org/10.1016/j.ijsolstr.2015.05.028>.
- Juhász, Z. and Szekrényes, A. (2015b), "Estimation of local delamination buckling in orthotropic composite plates using Kirchhoff plate finite elements", *Math. Prob. Eng.*, <http://doi.org/10.1155/2015/749607>.
- Jung, W.Y., Han, S.C., Lee, W.H. and Park, W.T. (2016), "Post-buckling analysis of laminated composite shells under shear loads", *Steel Compos. Struct.*, **21**(2), 371-394. <https://doi.org/10.12989/scs.2016.21.2.373>.
- Kaci, A., Houari, M.S.A., Bousahla, A.A., Tounsi, A. and S.R. Mahmoud, S.R. (2018), "Post-buckling analysis of shear-deformable composite beams using a novel simple two-unknown beam theory", *Struct. Eng. Mech.*, **65**(5), 621-631. <https://doi.org/10.12989/sem.2018.65.5.621>.
- Karami, B., Janghorban, M. and Tounsi, A. (2018), "Variational approach for wave dispersion in anisotropic doubly-curved nanoshells based on a new nonlocal strain gradient higher-order shell theory", *Thin-Wall. Struct.*, **129**, 251-264. <https://doi.org/10.1016/j.tws.2018.02.025>.
- Khayat, M., Poorveis, D. and Moradi, S. (2016), "Buckling analysis of laminated composite cylindrical shell subjected to lateral displacement-dependent pressure using semi-analytical finite strip method", *Steel Compos. Struct.*, **22**(2), 301-321. <https://doi.org/10.12989/scs.2016.22.2.301>.
- Khiloun, M., Bousahla, A.A., Kaci, A., Bessaim, A., Tounsi, A. and Mahmoud, S.R. (2019), "Analytical modeling of bending and vibration of thick advanced composite plates using a four-variable quasi 3D HSDT", *Eng. Comput.*, <https://doi.org/10.1007/s00366-019-00732-1>.
- Mahmoudi, A., Benyoucef, S., Tounsi, A., Benachour, A., Bedia, E.A.A. and Mahmoud, S.R. (2019), "A refined quasi-3D shear

- deformation theory for thermo-mechanical behavior of functionally graded sandwich plates on elastic foundations", *J Sand. Struct Mater.*, **21**(6), 1906-1926. <https://doi.org/10.1177/1099636217727577>.
- Matsunaga, H. (2005), "Thermal buckling of cross-ply laminated composite and sandwich plates according to a global higher-order deformation theory", *Compos. Struct.*, **68**(4), 439-454. <https://doi.org/10.1016/j.compstruct.2004.04.010>.
- Matsunaga, H. (2006), "Thermal buckling of angle-ply laminated composite and sandwich plates according to a global higher-order deformation theory", *Compos. Struct.*, **72**(2), 177-192. <https://doi.org/10.1016/j.compstruct.2004.11.016>.
- Meksi, R., Benyoucef, S., Mahmoudi, A., Tounsi, A., Bedia, E.A.A. and Mahmoud, S. (2019), "An analytical solution for bending, buckling and vibration responses of FGM sandwich plates", *J Sand. Struct Mater.*, **21**(2), 727-757. <https://doi.org/10.1177/1099636217698443>.
- Menasria, A., Bouhadra, A., Tounsi, A., Bousahla, A.A. and Mahmoud, S.R. (2017), "A new and simple HSDT for thermal stability analysis of FG sandwich plates", *Steel Compos. Struct.*, **25**(2), 157-175. <https://doi.org/10.12989/scs.2017.25.2.157>.
- Nikrad, S.F. and Asadi, H. (2015), "Thermal post-buckling analysis of temperature dependent delaminated composite plates", *Thin Wall. Struct.*, **97**, 296-307. <https://doi.org/10.1016/j.tws.2015.09.027>.
- Panda, S.K. and Singh, B.N. (2009), "Thermal post-buckling behaviour of laminated composite cylindrical/hyperboloid shallow shell panel using nonlinear finite element method", *Compos. Struct.*, **91**(3), 366-374. <https://doi.org/10.1016/j.compstruct.2009.06.004>.
- Park, T., Lee, S.Y., Seo, J.W. and Voyiadjis, G.Z. (2008), "Structural dynamic behavior of skew sandwich plates with laminated composite faces", *Compos.: Part B*, **39**, 316-326. <https://doi.org/10.1016/j.compositesb.2007.01.003>.
- Reddy, J.N. (2004a), *An Introduction to Nonlinear Finite Element Analysis*, Oxford University Press, Cambridge, UK.
- Reddy, J.N. (2004b), *Mechanics of Laminated Composite Plates and Shells: Theory and Analysis*, 2nd edition, CRC Press, Boca Raton, FL.
- Sadamoto, S., Tanaka, S., Taniguchi, K., Ozdemir, M., Bui, T.Q., Murakami, C. and Yanagihara, D. (2017), "Buckling analysis of stiffened plate structures by an improved meshfree flat shell formulation", *Thin Wall. Struct.*, **117**, 303-313. <https://doi.org/10.1016/j.tws.2017.04.012>.
- Semmah, A., Heireche, H., Bousahla, A.A. and Tounsi, A. (2019), "Thermal buckling analysis of SWBNNT on Winkler foundation by non-local FSDT", *Adv. Nano Res.*, **7**(2), 89-98.
- Shiau, L.C. and Kuo, S.Y. (2004), "Thermal postbuckling behavior of composite sandwich plates", *J. Eng. Mech.*, **130**(10), 1160-1167. [https://doi.org/10.1061/\(ASCE\)0733-9399\(2004\)130:10\(1160\)](https://doi.org/10.1061/(ASCE)0733-9399(2004)130:10(1160)).
- Singh, G., Rao, V.G. and Iyengar, N.G.R. (1993), "Thermal post-buckling behavior of laminated composite plates", *AIAA J.*, **32**(6), 1336-1338. <https://doi.org/10.2514/3.12143>.
- Singh, V.K. and Panda, S.K. (2014), "Nonlinear free vibration analysis of single/doubly curved composite shallow shell panels", *Thin Wall. Struct.*, **85**, 341-349. <https://doi.org/10.1016/j.tws.2014.09.003>.
- Srinivas, S. and Rao, A.K. (1970), "Bending, vibration and buckling of simply supported thick orthotropic rectangular plates and laminates", *Int. J. Solids Struct.*, **6**(11), 1463-1481. [https://doi.org/10.1016/0020-7683\(70\)90076-4](https://doi.org/10.1016/0020-7683(70)90076-4).
- Striz, A.G., Chen, W.L. and Bert, C.W. (1997), "Free vibration of plates by the high accuracy quadrature element method", *J Sound Vib.*, **202**, 689-702.
- Thankam, V.S., Singh, G., Rao, G.V. and Rath, A.K. (2003), "Thermal post-buckling behaviour of laminated plates using a shear-flexible element based on coupled-displacement field", *Compos. Struct.*, **59**(3), 351-359. [https://doi.org/10.1016/S0263-8223\(02\)00243-X](https://doi.org/10.1016/S0263-8223(02)00243-X).
- Wu, Y., Xing, Y. and Liu, B. (2018), "Analysis of isotropic and composite laminated plates and shells using a differential quadrature hierarchical finite element method", *Compos. Struct.*, **205**, 11-25. <https://doi.org/10.1016/j.compstruct.2018.08.095>.
- Yoshida, K., Sadamoto, S., Setoyama, Y., Tanaka, S., Bui, T.Q., Murakami C. and Yanagihara, D. (2017), "Meshfree flat-shell formulation for evaluating linear buckling loads and mode shapes of structural plates", *J. Mar. Sci. Technol.*, **22**(3), 501-512. <https://doi.org/10.1007/s00773-017-0433-2>.
- Zakeri, A.A. and Alinia, M.M. (2006), "An analytical study on post-buckling behaviour of imperfect sandwich panels subjected to uniform thermal stresses", *Thin Wall. Struct.*, **44**(3), 344-353. <https://doi.org/10.1016/j.tws.2006.03.001>.
- Zaoui, F.Z., Ouinas, D. and Tounsi, A. (2019), "New 2D and quasi-3D shear deformation theories for free vibration of functionally graded plates on elastic foundations", *Compos. Part B*, **159**, 231-247. <https://doi.org/10.1016/j.compositesb.2018.09.051>.
- Zarga, D., Tounsi, A., Bousahla, A.A., Bourada, F. and Mahmoud, S.R. (2019), "Thermomechanical bending study for functionally graded sandwich plates using a simple quasi-3D shear deformation theory", *Steel Compos. Struct.*, **32**(3), 389-410. <https://doi.org/10.12989/scs.2019.32.3.389>.
- Zhai, Y., Su, J. and Liang, S. (2018), "Free vibration and buckling analysis of composite sandwich plates in thermal environment", *J Sand. Struct Mater.*, <http://doi.org/10.1177/1099636218795375>.
- Zine, A., Tounsi, A., Draiche, K., Sekkal, M. and Mahmoud, S.R. (2018), "A novel higher-order shear deformation theory for bending and free vibration analysis of isotropic and multilayered plates and shells", *Steel Compos. Struct.*, **26**(2), 125-137. <https://doi.org/10.12989/scs.2018.26.2.125>.